Design of a Portable and Cost Effective Fat Measurement Sensor

John Chan You En, Chong Zheng Min Clarence, Teh Chee Yang

Introduction

Obesity is associated with a large number of diseases and metabolic disorders, such as type 2 diabetes, heart disease, high blood pressure, fatty liver disease, stroke, and some types of cancer. This is especially worrying in developed countries. In the USA, more than a third of adults aged 20 and above are considered obese [4]. Moreover, it is the fat stored in the abdominal cavity, also known as visceral fat, which contributes the most to increased health risks. [1] However, the existing non-invasive techniques of body fat measurement which can accurately determine the levels of visceral and subcutaneous fat are high-tech methods such as CT and MRI scans, and are very expensive. The most affordable form of body fat analysis which claims to be able to do this is Bio-electrical Impedance Analysis (BIA). However, BIA machines usually require electrodes to be placed at the extremities of the body, resulting in less accurate measurements. Furthermore, most BIA machines make use of the BMI, which requires a built in weighing scale, limiting the portability of the fat measurement device. [2]

In this paper, we propose a novel method of measuring the visceral fat percentage using electrodes placed in close proximity with the bulk of visceral fat (the abdominal region), to improve the portability and lower the cost of composite BIA devices.

With this objective, the following workflow process better illustrates the direction and scope of the project (see Fig 1). In this project, we hope to achieve phase 1 and begin phase 2 as we begin to characterise our sensor system and calibrate the data recorded to the human body. In future, our group hopes to be able to finalise the characteristic curve between human fat percentage and the measured data by our sensor system. Further analysis and calibration can be done in phase 3 where advanced technologies can be utilised to further enhance and identify the accuracy of our system.

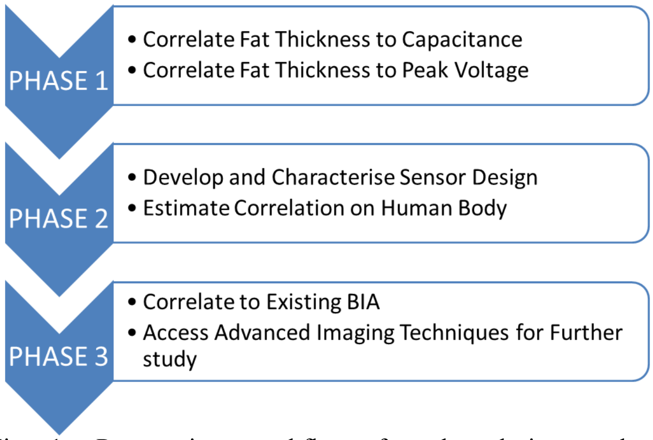

Fig 1: Progressive workflow for the design and development of the fat measurement design. Phase 1 would involve the correlation of fat thickness to capacitance and peak voltage. Phase 2 will lead to the potential realisation of the effectiveness of the sensor in detecting fat. Phase 3 will further improve the accuracy of the sensor by comparing its data to other more accurate and advanced techniques.

Prototype Sensor Design

Before getting immediately ambitious with creating a human fat sensor, it was necessary to first conduct tabletop experiments on animal fats and verify that a change in the thickness of fat causes a corresponding change in the measured electrical signal. The very first sensor has two separate acrylic plates, each lined with copper tape, and connected to an external RC circuit (see Fig 2a). Varying thicknesses of animal fat are sliced to size and inserted between the plates on the sides with copper tape, and a voltmeter reads out the potential difference across the plates at different modulation frequencies.

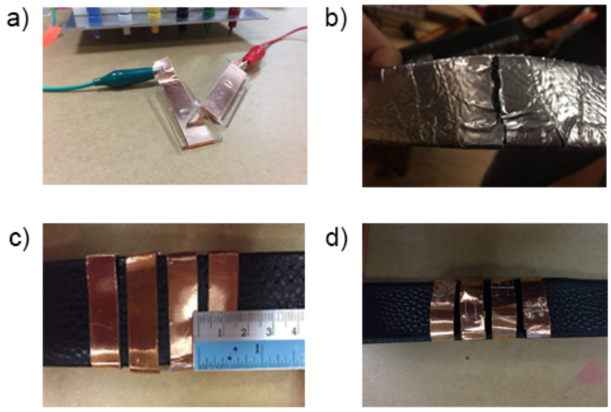

Fig 2: (a) sensor used in tabletop experiment (b) worn and torn aluminium tape (c) four pieces of copper tape wrapped around the belt width (d) the copper tapes are stapled in place

Before getting immediately ambitious with creating a human fat sensor, it was necessary to first conduct tabletop experiments on animal fats and verify that a change in the thickness of fat causes a corresponding change in the measured electrical signal. The very first sensor has two separate acrylic plates, each lined with copper tape, and connected to an external RC circuit (see Fig 2a). Varying thicknesses of animal fat are sliced to size and inserted between the plates on the sides with copper tape, and a voltmeter reads out the potential difference across the plates at different modulation frequencies.

After success with the table-top experiments, our next goal was to achieve a fat detection sensor that works on humans. Initially, the direct approach was to cover our belt with two very long pieces of aluminium tape surrounding the waist, separated by a few centimetres from each other. Whilst this created a very large capacitor area, this idea was, however, not successful because the relatively large distance between the sides of the waist resulted in a negligible capacitance. Furthermore, the aluminium tape was crumpled and lacerated after much wear and tear, thus indicating that it might not be durable for long term use (see Fig 2b). To improve the design, the aluminium tape was substituted with copper tape, which showed a lower degree of creasing. Additionally, instead of using the entire abdominal region as a dielectric for the capacitor, four closely separated strips of copper tape are stuck to the belt, serving as electrodes that contact with a small surface area just above the navel. This increases the measured capacitance and allows tremendous savings on the amount of material used.

To determine the physical dimensions, preliminary calculations are performed based on Equation 1:

$$C = \frac{\varepsilon A}{d} = \frac{\varepsilon W L}{d}$$

where C is the capacitance of fat
ε is the dielectric permittivity
A is the area of conductive tape
d is the separation between conductive tapes

Due to available material and ergonomic constraints, the width W of the conductive tape is 1.2cm, and d is set at 0.4cm (see Fig 2c). The copper tapes are stapled in place (see Fig 2d), but not at the contact point. For a rough estimate, let ε equal to the permittivity of free space. Research has also shown that the capacitance of a human body is in the range of 10^{-12} F [6]. By substituting these values into Equation 1, the required length L of the copper tape is:

$$L = \frac{(10^{-12})(0.004)}{(8.85\times10^{-12})(0.012)} = 0.037\text{m} = 3.7\text{cm}$$

This value of L is about equal to the width of an ordinary belt and hence, is suitably appropriate for the prototype sensor design. The circuit drawing of the sensor is shown in Fig 3. It comprises a Red Pitaya™ signal generator that generates a voltage across the electrodes at the furthest ends. Grounded probes are connected to each of the middle two electrodes to measure separate input signals when placed in contact with the skin. The quantifiable differences in amplitude and phase between both waveforms will provide information on the amount of fat inside the body.

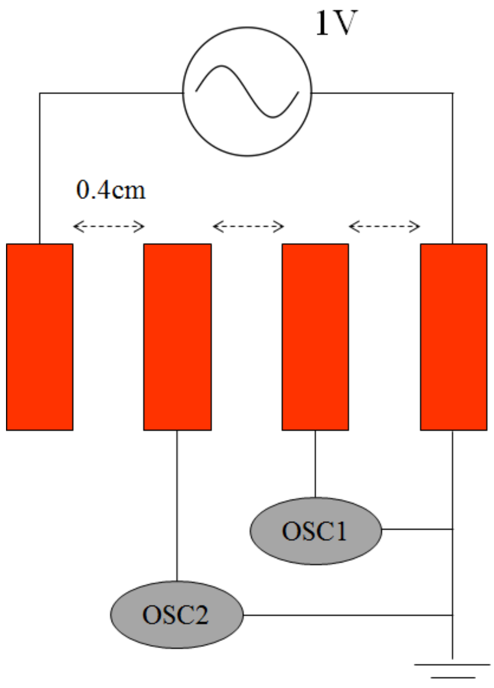

Fig 3: Schematic of the final sensor design with 4 probes. The first probe on the left will measure the output signal from the Red Pitaya while the second and third probe will measure IN1 and IN2 respectively, with the last probe connected to the ground.

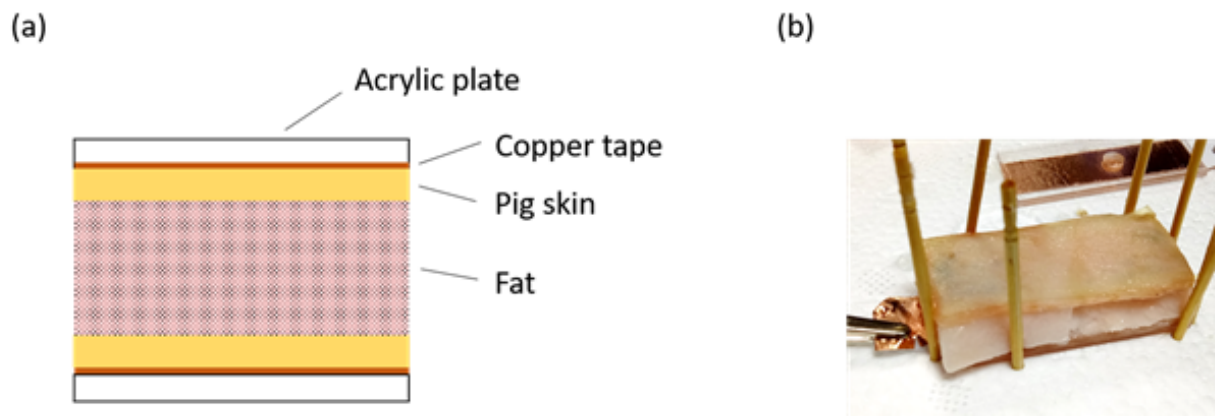

Fig 4: (a) schematic of capacitor (b) the actual capacitor in experiment that is designed to closely simulate the characteristic of the human body. This is done by sandwiching the fat samples with a layer of pork skin before it comes into contact with our sensor probes. Signal is then generated and sent to pass through the sample while the output voltage would be recorded.

Experimental Procedures

Table Top Experiment

In our project, the tabletop experiment was first carried out to finalise the proof of principle in our sensor design, confirming that the thickness of fat material will affect the capacitance value between our sensors. In this experiment, we aimed to simulate as close as possible to the human body.

Figs 4a & b illustrate the schematics of the experiment, showing the location of the acrylic plate that was lined with copper tape. A layer of pig skin was then used to line the target fat sample. The presence of the pig skin simulates the skin barrier that our sensor has to penetrate before it would receive signal from the fat tissues itself. Due to its wide availability in the supermarket, pig skin was chosen out of the several types of animal skin. The fat samples chosen were pork fat and butter for us to identify the presence or difference in capacitance in this two sample types. The fat samples were then cut according to the thickness of interest. In the case of pork fat, it was bought from the supermarket and came in smaller bits and pieces. In order for us to vary the thickness significantly, we stacked the fat samples horizontally so as to reduce air gaps in the vertical direction, between the two sensor plates. The actual experimental setup can be seen in Figure 1b. Toothpicks were used to surround the sample to prevent the tautness of the wiring cable to shift the skin and fat position away from its original position.

The results obtained, as shown in Fig 5a with the use of pork fat and skin as described earlier, showed that there was indeed a change in peak output voltage value recorded. It can be seen that when fat is added in between the pig skin, the peak voltage is higher by approximately 25V with 10mm of fat sample tissues as compared to just skin without fat samples. This is crucial in determining that there is indeed a capacitive value present in fat tissues which led to the increase in output voltage recorded as voltage drop across the sensor probes increase. This drop signifies that there was some sort of impedance present in the tissue samples, in this case the capacitance of the fat tissues. However, there may be some instability in the test structure, leading to an unclear trend at larger thicknesses. The sensor was held in place by placing a

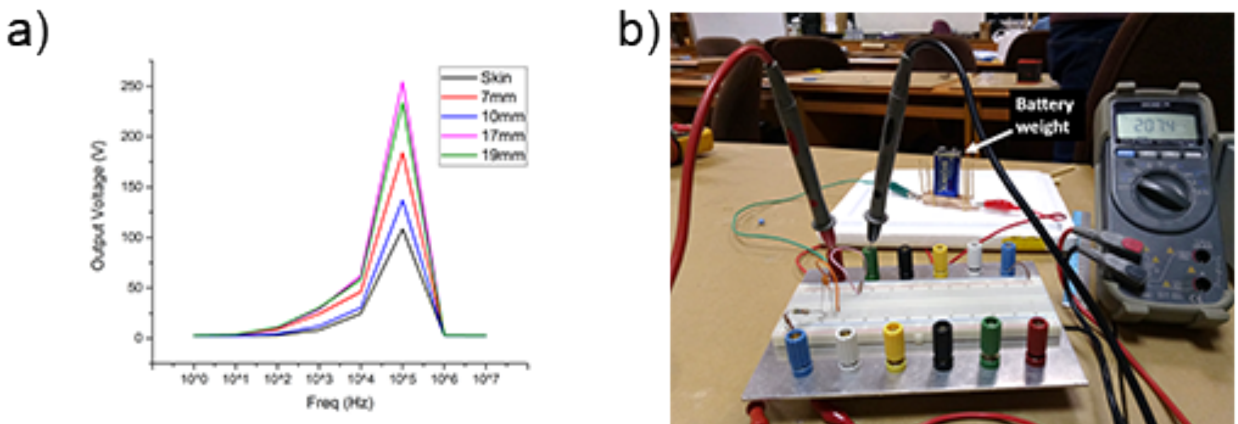

Fig 5: (a) results from tabletop experiment showing peaks in the output voltage recorded during the tabletop experiment using pork fats as the sample. Different thickness of fat appeared to have resulted in different peak values, suggesting that there is a change in capacitance with thickness. (b) experimental setup to illustrate the instability of the probe's placement thus the need of placing a battery weight onto the sample so as to secure its position.

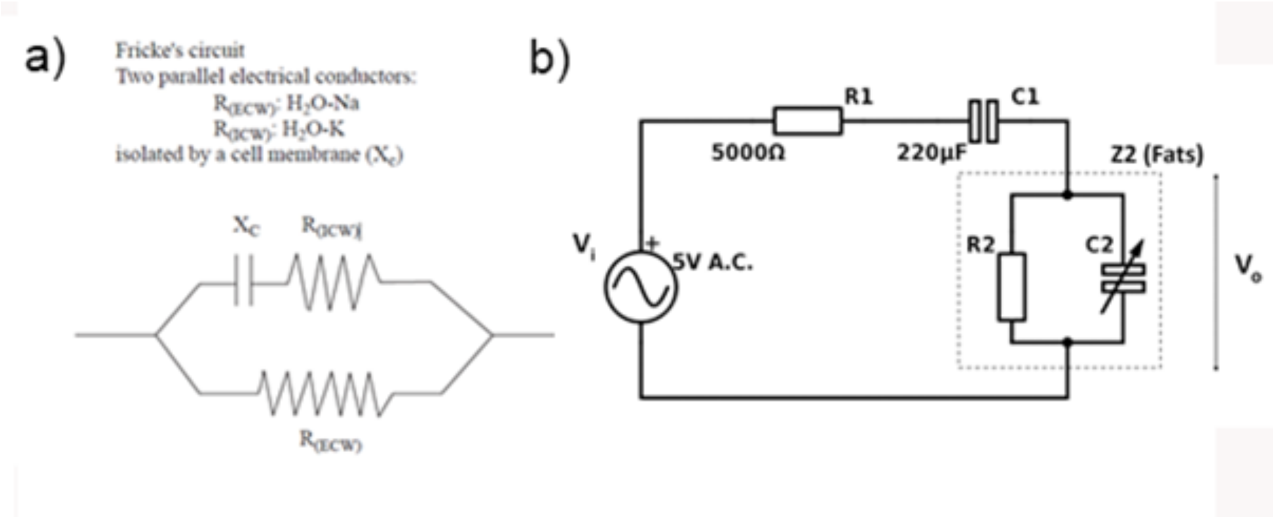

Fig 6: (a) model of the human body (b) circuit used to simulate the model that suggests the presence of resistance and capacitance in the human body

battery weight on top as shown in Fig 5b. Despite the instability in the setup, there is still a conclusive result that with added fat samples in between the skin, capacitance was detected at significant and readable values.

Research has shown that the human body possesses both resistive and capacitive characteristics [3]. This was portrayed with respect to Fig 6a, where the human body is represented as a capacitor in series with the resistive value of Intra-Cellular Water (ICW). The resistive value of Extra-Cellular Water (ECW) is placed in parallel with the other capacitive and ICW resistive characteristic. For us to utilise this electrical model for our project, we first have to perform a small scale exercise to determine if our bodies have the aforementioned capacitive and resistive characteristics. This experiment was carried out by setting up our sensor, made by a large strip of aluminium tape, which was attached onto a belt. The initial circuit schematic for our sensor design is shown in Fig 6b, where resistance and capacitance was added into the circuit. The values chosen were determined by the order of magnitude of capacitance and resistance in the human body. The belt was carefully placed across the abdomen, maintaining a three finger spacing above the navel. A measurement of output voltage was measured across the sensor probes. In this experiment, the sensor probes are connected in series to a set of capacitance of different orders, ranging from nF to uF. This setup was used to identify the presence of capacitance on our body. With the signal generator provided by the Red Pitaya™, we were able to determine that there was a drop in signal between the output and the input readings with the various order of capacitance, with 100uF achieving almost half the drop in peak voltage recorded. This is done similar to identify the presence of resistance, with the replacement of the capacitor with resistors and the signal generator set to D.C. Mode. Similar a MΩ resistor resulted in a 50% decline in peak voltage. The experiment was repeated with different subjects so as to remove any systematic error or exclusivity. This experiment concluded that the human body possesses capacitive characteristics at the orders of 100uF and resistance at approximately Mohms. Thus, the table-top experiments that were carried out determined that fats indeed has capacitive properties and that our human body possesses both capacitive and resistive properties.

Final Sensor Design Experiment and Setup

Following the tabletop experiment on the different kinds of fat, we designed an experiment to record the variations in voltage and phase difference between IN1 and IN2 when a potential difference was generated across OUT1 and GRD. The Red Pitaya Digital Oscilloscope from STEMlab was used in order to generate voltage signals with frequencies ranging from 0HZ (DC) to 10MHz via channel OUT1. Channels IN1 and IN2 were connected back to the Red Pitaya to be displayed on the digital oscilloscope. The .csv files were subsequently exported to LabVIEW and analysed for the difference between the peak-to-peak voltages, as well as the phase difference between the two waveforms IN1 and IN2.

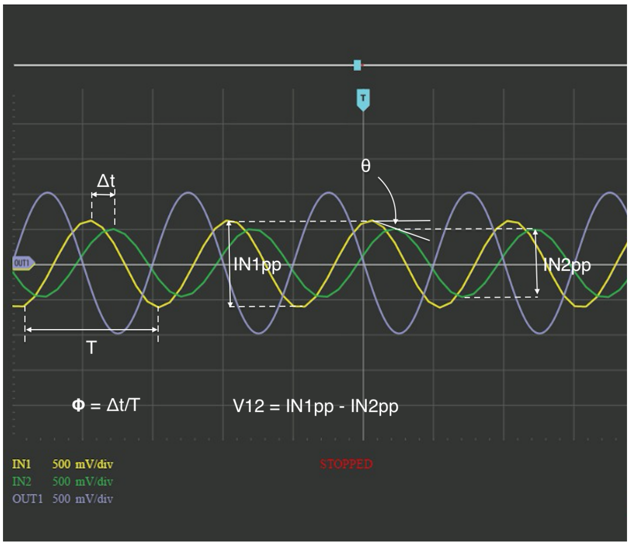

Fig 7: Definitions of variables and the waveforms as seen on the Red Pitaya.

Experimental procedure:
1) Take subject's body fat percentage reading on BIA device
2) Set up electrodes as shown in Fig 8 on a human body
3) Ensure that electrodes are 3 fingers' spacing above the navel
4) Tighten belt so that skin is in firm contact with electrodes
5) Generate voltage signal via OUT1
6) Scale graph shown on Red Pitaya and save .csv file
7) Run .csv file through LabVIEW code to obtain $V_{12} = IN1_{pp} - IN2_{pp}$ and phase difference between IN2 and IN2
8) Compare results with body fat percentage reading to obtain a correlation between the fat percentage and the phase shift or peak voltage difference

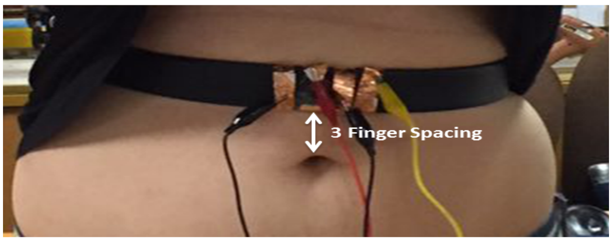

Fig 8: Placement of sensor probe on human body, ensuring that it is placed 3 fingers above the navel so as to take data from this region of interest only

This experiment was carried out across four individuals with body fat percentage ranging from 15% to 20%, two individuals with body fat percentage ranging from 20% to 25%, and two individuals with body fat percentage >25%. Due to time constraints, additional subjects could not be tested.

Results and Discussion

Results from the different modulation frequencies used (0Hz-10MHz) were compared, and the frequency with the most similar effect on the individuals with 15-20% body fat (10MHz) was selected so that any deviations from the mean would be detected easily. This can be seen in Figure a-d below, where the amplitudes and phase differences of the waveforms do not appear to be significant for frequencies 1kHz to 1MHz. This is in comparison with 1e7 in Fig 7, where a very noticeable phase difference and voltage difference can be observed.

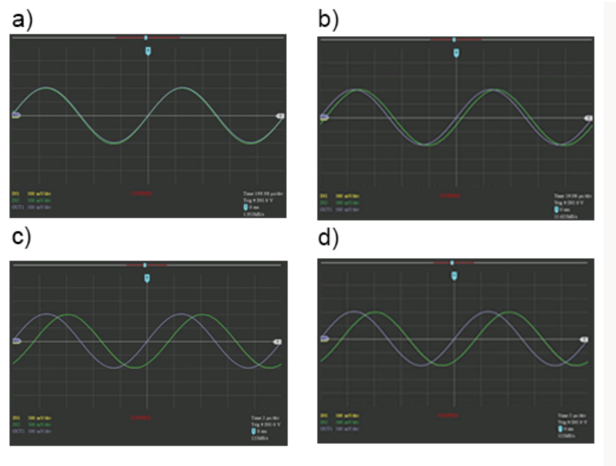

Fig 9: Signal response from Red Pitaya registering the output signal (Grey), IN1 signal (Yellow) and IN2 signal (Green) at the respective frequency (a)1kHz (b)10kHz (c)100kHz (d) 1MHz

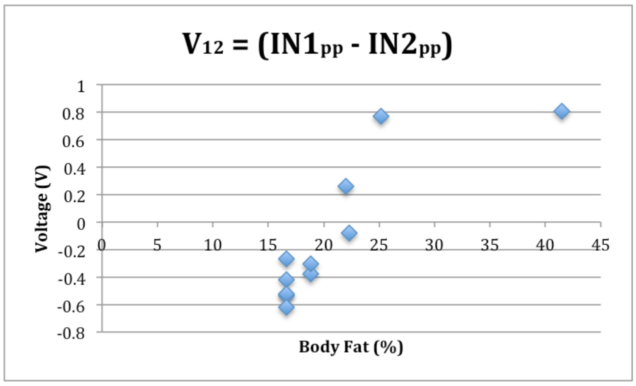

Fig 10: Scatter plot of the peak to peak voltage difference between channels IN1 and IN2 (V_{12}) vs body fat percentage of the different individuals at a frequency of 10MHz.

A scatter plot of the results for f = 10MHz is shown in Fig 10. A total of 11 readings were recorded. By regression and interpolation, it is apparent that the values obtained from the experiment are described by either a logarithmic curve or a linear curve with a saturation voltage. While the relationship between body fat percentage and peak to peak voltage difference remains unclear, it can be seen that at lower fat percentages (15-20%), the values do not deviate much from each other. Additionally, whether it is a logarithmic or linear curve, the values seem to be linear around the 15-25% range, which shows that there is a useful correlation between our sensor and the conventional BIA device used.

However, at higher values of percentage body fat, the peak voltage difference V_{12} is much larger than that of lower body fat values, and hence a clear distinction can be drawn between individuals with higher body fat percentage vs individuals with lower body fat percentage.

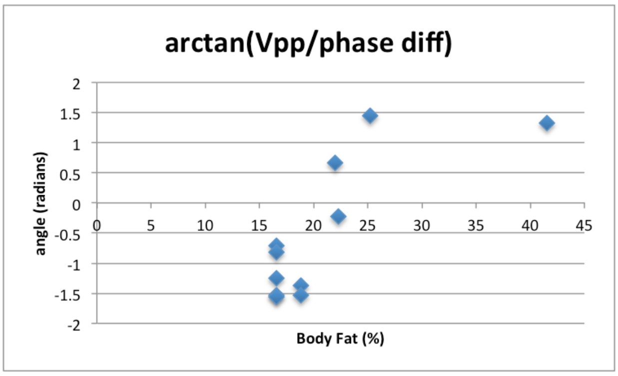

Fig 11: The peak to peak angle, $\theta = \arctan(\Delta Vpp/\Delta\phi)$, defined in Figure X. It is calculated by taking the inverse tangent of the difference in peak to peak voltage divided by the phase difference. Modulation frequency f = 10MHz.

As shown in Fig 11, the angle θ also seems to be correlated to the change in fat percentage detected by the conventional BIA machine. Though the spread of values differs slightly from Fig 10, a linear correlation can also be observed from 15-25% body fat, and a logarithmic or linear-saturated relationship may characterize the curve. This curve may also be used as a comparison to the curve in Fig 10, and be used as a fail-safe when fat percentage is estimated.

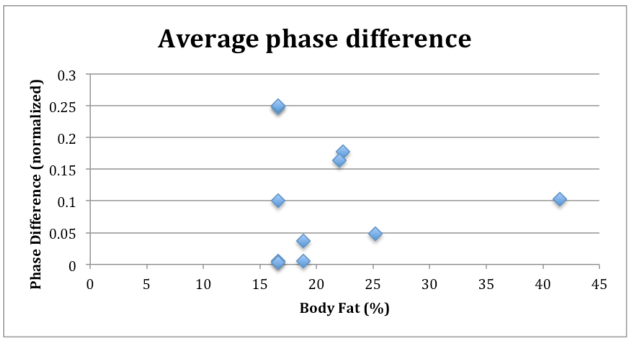

Fig 12: A scatter plot of the phase difference between channels IN1 and IN2, at f = 10MHz. Phase difference is calculated by taking the average of the time difference between the peaks and troughs of different waves, divided by the period (See Fig 7).

However, there are certain parameters that did not show any positive correlation, such as average phase difference and body fat percentage as seen in Fig 12. The data analysed clearly showed no relationship that can be estimated to be linear. As a result, the processed data to identify phase difference between IN1 and IN2 did not prove to be a viable dataset in the characterising the sensor. Thus, we have identified and isolated phase difference measurements so as to prevent obtaining a false positive or false negative result.

Advantages of Newly Designed Sensor

Competitive Pricing

An accurate, commercial BIA sensor from Tanita costs about USD6000. In contrast, our sensor saves almost 10 times in expenditure, as it would cost only around USD450, of which the Red Pitaya™ is USD420. A more customizable integrated circuit could be used to further reduce the cost of production.

Closer Proximity to Visceral Fat

With a belt like design, our sensor is able to bypass the arms and legs and measure visceral and subcutaneous adipose tissue at the abdominal region more directly, with greater proximity. Conventional BIA devices which use BMI to estimate the body fat percentage in an individual usually have electrodes located at the extremities of the body, and hence may not return an accurate value of visceral fat, which is the harmful fat surrounding one's organs. Rather, they usually measure subcutaneous fat and visceral fat combined with fat along the arms and legs are also taken into consideration. However, vital organs are only affected by the presence of visceral fat, rendering the measurement of subcutaneous fat to have less significance in its effects on the health of a person. As a result, it is important to note that the additional measurement of subcutaneous fat as done by the BIA device, might incur additional systematic error in its measurements and estimations. Our fat sensor device on the other hand, confines the signal sent to be within a small region of interest, mainly across the abdominal area where most vital organs are located. By isolating the region of interest in this case, we would be able to potentially reduce systematic errors in our estimation with the lesser area of measurements involved. Thus, our sensor has the potential to measure visceral fat more accurately as compared to conventional BIA devices.

Portable

With the Red Pitaya weighing only a few hundred grams, this sensor design has the potential to be more accurate yet more lightweight and portable than any other BIA measurement device. Owing to the fact that most BIA measurement devices use BMI, a weighing scale has to be incorporated into the design, which often makes the device bulky and heavy. By isolating our region of interest to only the abdominal area allowed the design of the sensor to be more compact. Together with the Red Pitaya, portability was one of the main highlights in our design. With the probes attached to a waist belt, it can be easily folded and put aside. It can be brought around easily with its compact size as compared to professional BIA devices, thus improving the portability of the fat sensor device that we have designed.

Future Work

Improving Conductivity

While our team has shown that the current prototype sensor design is fully functional, there are still areas which can be improved to make the final product more robust. For example, one problem faced was poor contact between the copper tape and skin, resulting in an intermittent signal. For even stronger contact, an adhesive layer that sticks well to skin should be added onto the belt so that there will be a lower impedance mismatch. This can be done using ECG gels that are readily available in most hospitals and pharmacies. Other than increasing the modulation frequency beyond 10MHz, ways to expand the sensor's fat sensitive range need to be further investigated.

Better Correlation

Due to time and manpower limitations, our collected data lacked a sufficiently large sample size for general deductions to be made. As such, more data is needed to be collected over a wider sample spread and more experiments carried out to determine the repeatability of the results. With more data, the standard deviation and mean of the data population can be better and more accurately determined. This would also determine the sensitivity of the sensor and also the limit range of the system.

In addition to statistical improvements, the sensor can also be correlated to more accurate fat measurement sensors such as dual X-rays and MRI systems that have the highest accuracy in fat detection within the human body in contemporary medical screening technology. Commercial BIA systems have their limitations in accuracy due to its technique and approach in measurement. As such, these limitations would implicate the results in comparing our sensor system with current commercial BIA devices. By comparing our collected data with these more accurate machines such as MRI and dual X-ray systems, we would be able to further determine the accuracy and error range of our sensor design and act on further improvements. Advanced imaging techniques are also able to accurately identify the presence and quantification of visceral fat. With further investigations using these equipments, we would be able to further correlate and characterise our sensor system's ability of detecting and quantifying the presence of visceral fat along the targeted region of interest. One limitation that we might face in doing this comparison is the availability and cost involved in utilising these equipment for calibration and characterization purposes of our sensor.

Wireless Capabilities

To further improve the portability of the sensor device, wireless capabilities can be implemented into the design so as to remove the presence of wires in the system. The latest prototype fat sensor system requires the use of large wires to carry the signals from the Red Pitaya to the sensor system. The Red Pitaya is also wired to the laptop for data acquisition, adding more weight into the overall system. We aim at adding a Bluetooth connection feature into the system for the Red Pitaya to wirelessly transmit data to the laptop. In addition, a phone application can be designed as well for future improvements in portability, where data can be transferred to the phone directly, making the use of a laptop to be redundant. These improvements would potentially improve the portability of the sensor device, allowing greater ease in monitoring fat in their bodies and various user benefits such as remote fitness monitoring by fitness instructors.

Conclusion

This paper has found that a high modulation frequency of 10MHz is effective for detecting fat in the human body. It has proposed a fully functional and relatively inexpensive sensor design that is characterized by linear voltage response in the range of 15-25% of fat by composition. The voltage difference between two input signals is directly related to the the amount of body fat, but no distinct trend is observed for the phase difference.

References

[1] Kooy K. V. D. Seidell J. C. Changes in body composition and fat distribution in response to weight loss and weight regain. -, 1993.
[2] G. Sergi M. Bussolotto P. Perini I. Calliari V. Giantin A. Ceccon F.
Scanferla G. Moschini G. Enzi. Accuracy of bioelectrical impedance analysis in estimation of extracellular space in healthy subjects and in fluid retention states. *Department of Internal Medicine*, 1994.
[3] U.Kyle.Bioelectricalimpedanceanalysisparti:Reviewofprinciples and methods. *Clinical Nutrition*, 2004.
[4] National Institute of Diabetes, Digestive, and Kidney Diseases. Overweight and obesity statistics. (n.d.). -, 2017.
[5] J Petrofsky. The effect of the subcutaneous fat on the transfer of current through skin and into muscle. -, 2008.
[6] O. Fujiwara and T. Ikawa. Numerical calculation of human-body capacitance by surface charge method. Electronics and Communications in Japan (Part I: Communications) 85(12), pp. 38-44. 2002. DOI: 10.1002/ecja.10025.

Acknowledgements

We would like to extend our greatest gratitude to A. khursheed, I. Raisul and N. karupiah for their invaluable feedback and advice in the duration of the project, without whom we would not be able to proceed.

Appendix

LabVIEW Pseudocode

BEGIN
Read from .csv file.
Separate .csv file into 4 arrays: Time, IN1, IN2 and OUT1.
FOR arrays IN1 and IN2,
    Detect the first peak and first trough of the array, ignoring noise by discarding values if dV/dt changes sign convention for any of the past 3 values.
    Detect voltage of first peak and first trough in the array
    Record the index of the element (array indices are used instead of time) in the array.
ENDFOR
$IN1_{pp}$ = Peak(IN1) – Trough(IN1)
$IN2_{pp}$ = Peak(IN2) – Trough(IN2)
V_{12} = $IN1_{pp}$ – $IN2_{pp}$
Phase difference = {[|Peakindex(IN1) – Peakindex(IN2)|]
    + [|Peakindex(IN1) – Peakindex(IN2)|]} / 2
Display waveform graph of IN1, IN2 and OUT1
END

LabVIEW Front Panel

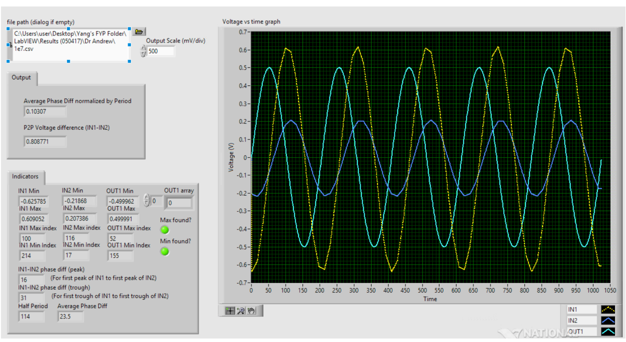

LabVIEW Code for First Minimum

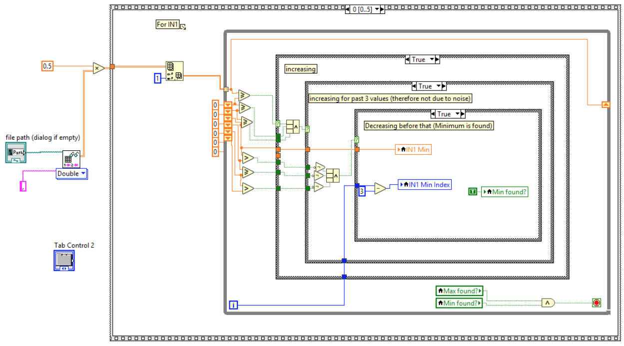

LabVIEW Code for First Maximum

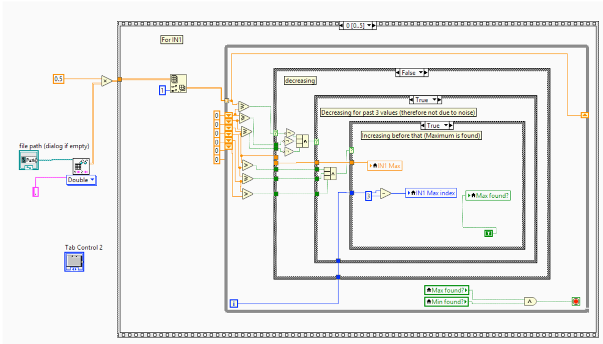

Calculation of Voltage Difference

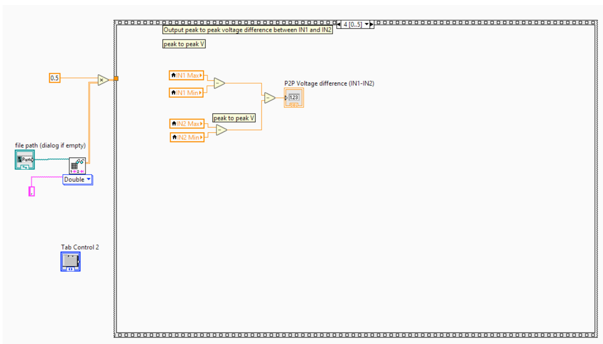

Calculation of Phase Difference